Laser and Particle Beams (2006), *24*, 101–106. Printed in the USA.

DOI: 10.1017/S0263034606060150

Experimental prospects at the Canadian advanced laser light source facility

T. OZAKI, J.-C. KIEFFER, R. TOTH, S. FOURMAUX, and H. BANDULET
Université du Québec, Institut National de la Recherche Scientifique, Varennes, Québec, Canada
(Received 17 June 2005; Accepted 18 September 2005)

Abstract

We describe here the present status of the Advanced Laser Light Source (ALLS) facility, a state-of-the-art multi-beam Ti:sapphire laser system presently under construction in Canada. ALLS is a national user facility to be commissioned in 2005 at the INRS campus near Montreal. The 25 fs ALLS multi-beam laser system has three components, each with different repetition rate and output energy. These multiple laser beams will be used to generate a "rainbow" of femtosecond pulses from the far infrared to hard X-rays, which can be combined to perform unique experiments, such as dynamic molecular imaging. In this paper, we describe two examples of experiments that are planned by our group with the ALLS facility. The first is the highly efficient generation of high-order harmonics using ablation medium. We demonstrate the generation of up to the 53^{rd} harmonics ($\lambda = 15$ nm) of a Ti:sapphire laser pulse (150 fs, 10 mJ), using pre-pulse (210 ps, 24 mJ) produced boron ablation as the nonlinear medium. The second example is the demonstration of in-line phase-contrast imaging with an ultrafast (300 fs) laser-based hard X-ray source (Mo K-α line). Images of biological samples have shown great enhancement of contrast due to this technique, distinguishing details that are barely observable or even undetectable in absorption images.

Keywords: Dynamic molecular imaging; Femtosecond lasers; High-order harmonic generation; X-ray imaging

1. INTRODUCTION

The Canadian community is establishing at the Institut National De La Recherche Scientifique (INRS) near Montreal, a Canadian based International Research Facility that will explore a completely new approach to investigation of matter. The facility, named the Advanced Laser Light Source (ALLS), will be a central facility open to users from various horizons, from universities, governmental laboratories, and industries. The ALLS scientific program includes several applications that require a truly multidisciplinary effort, combining the expertise of physicists, chemists, physicians and biologists. ALLS will extend frontiers of light and particle sources needed for time resolved experiments or imaging applications.

The mission of the ALLS program is to establish a user facility that will cluster Canadian institutions and international partners from different sectors and disciplines. The central facility will strongly interact upstream with the intermediate scale laboratories specialized in different areas of research and doing system development, and downstream with the user teams and laboratories working on applications in various disciplines.

The central concept of ALLS is to use a plurality of laser interactions, spanning the X-ray to infrared (IR) spectral ranges, with sufficient peak power to manipulate matter at will and probe its dynamics. The ALLS workhorse is a new state-of-the-art multi-beam laser system, which is making use of the most recent ultrafast Ti:sapphire laser technology (Keller, 1994; Nisoli *et al.*, 1998; Backus *et al.*, 2001; Cerullo & De Silvestri, 2003; Kuroda *et al.*, 2005). The various light sources will compose a multi-beam *femtosecond "rainbow"* system that will deliver high photon fluxes with extremely short duration pulses at various wavelengths. In the IR (8–10 μm) there will be a beam line for molecular manipulation and studies. An intermediate IR and visible (0.5–3 μm) beam line will be used for the control of molecular reaction dynamics and alignment. A third beam line in the vacuum ultraviolet (VUV) and soft X-rays (10–200 nm) will be devoted to characterizing energetics and ultrafast electron dynamics. A fourth beam line will be used to create powerful attosecond pulses in the soft X-ray spectral range. The fifth beam line will be for generating photons in the hard X-ray range and will be used for femtosecond

Address correspondence and reprint requests to: Tsuneyuki Ozaki, Université du Québec, Institut National de la Recherche Scientifique, 1650 Boul. Lionel-Boulet, Varennes, Québec J3X 1S2, Canada. E-mail: ozaki@emt.inrs.ca

X-ray diffraction and femtosecond EXAFS and XANES measurements. This beam line will also be heavily integrated with high field studies of plasma formation and associated physics. Construction of the laser and beam lines started in mid-2003, and the infrastructure will be fully operational by mid-2006. Various beam lines are progressively implemented and parts of the ALLS will be available for users at the end of 2005.

The ultimate goal of the ALLS project is to measure the structure of non-crystallizable molecules (proteins) and open a route to understanding the dynamics of various molecular reactions. A number of exciting new concepts will be explored with ALLS in the generation of attosecond light pulses, femtosecond duration X-ray, and electron sources, coherent X-ray sources, high-energy electron, and ion sources, short lived isotopes for medical procedures such as positron emission tomography and other high field plasma based phenomena. Potential applications in various domains of the ALLS secondary sources include science on the ultimate time scale, and quantitative imaging of molecules, clusters, solids, and biological systems. The ALLS facility is also the tool to explore unprecedented states of matter involving relativistic nonlinearities.

Part of the same beam output will feed high-energy optical parametric amplifiers (OPA). The OPA systems produce the usual signal and idler beams but also includes a large assortment of frequency conversion crystals, which allows the unit to cover, in different bands, a large spectrum from the UV (250 nm) to the far IR (20 μm). These beams are available for measurements such as pump-probe measurements and resonant excitation.

Experiments will be set up to accommodate an excitation pulse from a variety of available wavelengths and any combination of probe wavelengths covering the entire UV to mid-IR. Similarly, high harmonic generation will lead to both pump and probe wavelengths in the soft X-ray to VUV range.

2. ABLATION HARMONICS

The generation and application of high-order harmonics are some of the major objectives of our group with the ALLS facility. High-order harmonics generated from the interaction of ultrashort laser pulses with gas jets and solid targets has proven to be an effective source of coherent short-wavelength radiation and attosecond pulses (Macklin *et al.*, 1993; Spielmann *et al.*, 1997; Seres *et al.*, 2004; Norreys *et al.*, 1996; Pascolini *et al.*, 2004). Molecular systems are also presently under consideration (Flettner *et al.*, 2003), due to their enhanced nonlinear susceptibility. Meanwhile, ablation generated by laser-solid interaction has long been considered as a medium for frequency conversion in various schemes (Akiyama *et al.*, 1992; Ganeev *et al.*, 1997). However, the maximum observed harmonic order generated at these conditions was limited to 11th (Ganeev *et al.*, 1997) and 13th (Akiyama *et al.*, 1992), and no plateau was observed in these studies.

Here we present our studies on harmonic generation from boron ablation, irradiated by a femtosecond pulse. Harmonics up to 53rd order (15 nm wavelength) were observed and the influence of various parameters on frequency conversion efficiency was analyzed. The steep decrease in the conversion efficiency for low-order harmonics (up to 19th) was followed by a long plateau. This is the first demonstration of a plateau in the harmonic spectrum from ablation plume.

The pump laser used in this work is a commercial, chirped pulse amplification Ti:sapphire laser system. A portion of the uncompressed radiation (24 mJ, 210 ps, 796 nm center wavelength) is split from the main beam by a beam splitter, which is used as the prepulse. This prepulse is focused onto a 5-mm-thick boron slab target using a spherical lens (Fig. 1). The spot diameter of the prepulse at the target surface was adjusted to be 600 μm, and the intensity of the prepulse on the target I_{pre} was between 2×10^{10} to 1×10^{11} W cm^{-2}. After a delay time, the femtosecond main pulse (10 mJ, 150 fs) irradiates the boron ablation from the longitudinal direction, using a 200 mm focal length lens. The maximum intensity of the main pulse I_m is 5×10^{15} W cm^{-2}. The delay between the main pulse and prepulse for this experiment was 18 ns. The generated harmonics were spectrally dispersed using a flat-field grazing incidence extreme ultraviolet (XUV) spectrometer with the Hitachi 1200 grooves/mm grating (Ganeev *et al.*, 1997). The XUV spectrum is detected by a micro-channel plate (MCP) with a phosphor screen, and recorded using a high-sensitivity CCD camera.

We used a flat-field soft X-ray spectrometer for the analysis of frequency conversion in the spectral range between 5 and 60 nm. High harmonics up to 53rd (15 nm) were observed in these experiments (Fig. 2a). The harmonics generated from the boron ablation appeared to be similar to those observed in gas harmonics, with characteristic plateau for harmonics exceeding 21st order (Fig. 2a). The conversion efficiencies were in the range of 10^{-4} (for third harmonic) to 10^{-7} (for harmonics in the plateau) (Fig. 3). The plateau disappeared when the prepulse energy was increased, which generated a continuum from the prepulse-produced boron ablation (Fig. 2b). In this case, the highest harmonics observed was the 19th order. When the prepulse energy was further increased, spectral lines from singly ionized and multiply ionized B ions appeared in the spectrum (Fig. 2c), in which case we did not observe any harmonics with wavelengths shorter than 65 nm.

The picosecond prepulse plays a crucial role in the creation of the optimal conditions for harmonic generation. For relatively small prepulse energies the harmonic intensity scaled as I_m^{γ}, with γ ranging between 3 to 5. However, with further growth of pulse energy (above 10 mJ, corresponding to a prepulse intensity $I_{pre} > 5 \times 10^{10}$ Wcm^{-2}) there was a saturation (in the case of the 3rd and 9th harmonic), or even considerable decrease of harmonic intensity (in the case of

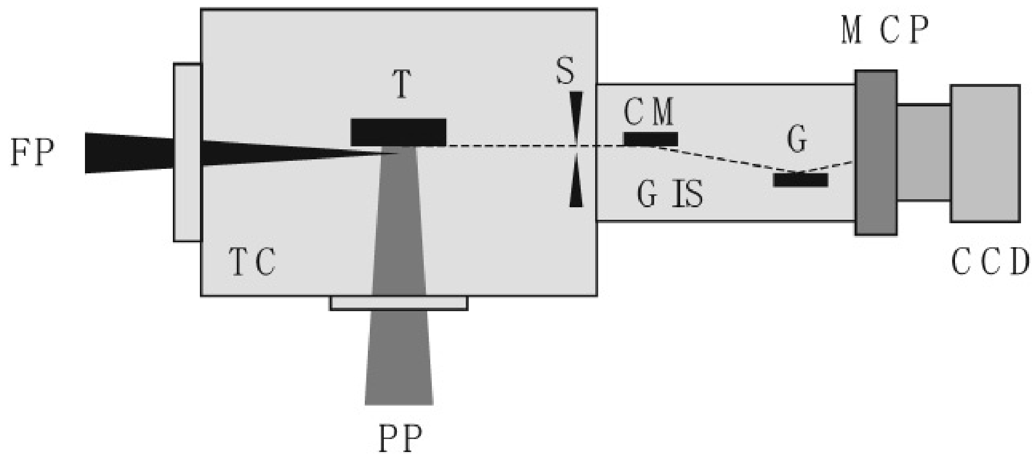

Fig. 1. Schematic diagram of the experimental setup for high-order harmonic generation. TS: target chamber; T: target; S: slit; CM: gold-coated cylindrical mirror; GIS: grazing incidence spectrometer; MCP: micro channel plate; CCD: charge coupled device; FP: femtosecond pulse; PP: picosecond pulse.

the 31st harmonic). We can explain the nonlinear increase in the harmonic intensity with prepulse intensity I_{pre} as the result of the increase in the particle density with I_{pre}. It has been shown that the harmonic yield has a quadratic dependence on the particle density in the plateau region (Reintjes, 1984; Altucci *et al*., 1996). The saturation of frequency conversion can be attributed to processes such as phase mismatching and ionization-induced defocusing of the main pump beam (Altucci *et al*., 1996), both of which are due to the production of free electrons in the ablation plume.

We investigated the harmonic yield as function of the polarization of main pulse. Both linear p- and s-polarization showed equal conversion efficiency of harmonic generation, while in the case of circular polarization no harmonics were observed. The optimal conditions for harmonic generation were found to be at the distance to 50–100 μm from the target surface, depending on harmonic order. This distance was found to be longer for the lower-order harmonics. No harmonics were observed when the picosecond pulses were used as both prepulse (60 mJ, 210 ps) and main pulse (70 mJ, 210 ps). We did not observe any changes in the spectrum of the main pump pulse after propagation through the plasma in separate experiments up to the intensity of $I_m = 8 \times 10^{15}$ Wcm^{-2} when a breakup of spectrum was caused, probably due to self-phase modulation. We did not observe any spectral shift of harmonics.

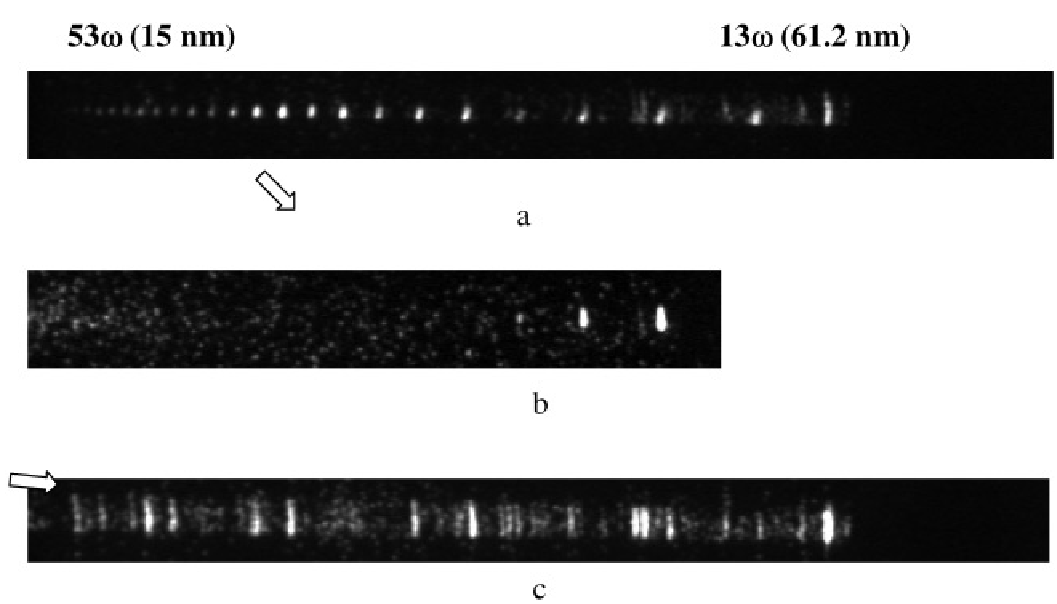

Fig. 2. Harmonic spectra in the cases of (**a**) low-excited boron plasma, (**b**) continuum generation, and (**c**) boron spectral lines in the case of strong excitation.

https://doi.org/10.1017/S0263034606060150 Published online by Cambridge University Press

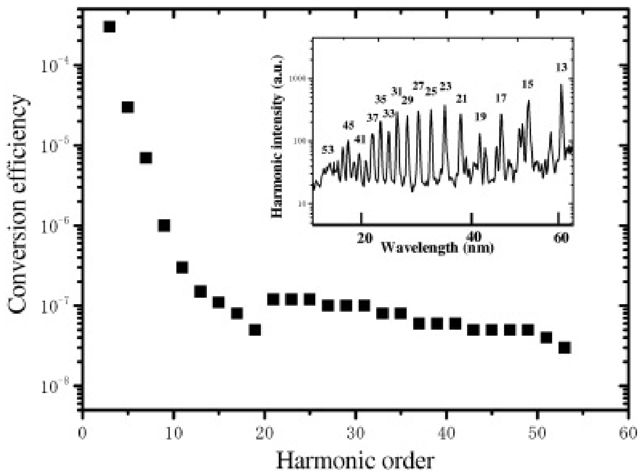

Fig. 3. Efficiency of harmonics generated in boron plasma. Inset is the harmonic yield in the wavelength range of 15 nm to 60 nm.

The mechanism of high-order harmonic generation with ablation medium can be inferred from two of our experimental observations. The first is the observation of only odd harmonics, and the second is the strong dependence of the harmonic intensity on the polarization ellipticity of the pump beam. Both are typical characteristics of gas harmonics, whose mechanism is well explained by the so-called Simple man's model (Corkum, 1993). According to this model, a linearly polarized high-intensity laser pulse irradiates an atom, and the high electric field of this laser distorts the Coulomb potential holding the bound electron to the atom. As a result, a portion of the bound electron wave function tunnels through the barrier produced by the combined effects of the laser electric field and Coulomb potential, thereby resulting in ionization (tunneling ionization). The ionized electron is then driven by the electric field, and when the direction of the electric field changes, the electron recollides with the parent ion. If this recollision results in radiative recombination, the ultrafast process results in harmonic radiation.

We have also observed that over-ionization of the preplasma up to the second ionization stage resulted in a complete disappearance of the harmonics, which indicates that harmonics are generated mainly by neutral and singly-ionized atoms.

The use of solid target ablation for high harmonics generation has several advantages compared to gas jets (for example, simplicity, gas saving, no differential pumping). The target degradation in our experiments was not observed until after several hundred shots in the case of high excitation, which resulted in a decrease in the conversion efficiency in the plateau range. However, after optimization of experimental conditions we were able to observe very stable generation of high-order harmonics without the necessity of changing the target position. This property will allow harmonic generation at kHz-repetition rate that allow increased average power of XUV harmonics.

3. X-RAY PHASE CONTRAST IMAGING

Another set of experiments that is of interest for our group is X-ray phase-contrast imaging (Wilkins *et al.*, 1996; Gureyev *et al.*, 2001), which is an emerging new technology for improved low-contrast resolution in biomedical imaging. The in-line geometry requires only an X-ray source (Gavrilov *et al.*, 2004; Limpouch *et al.*, 2004) with a very small effective focal spot size, a suitable spectral distribution, and an appropriate location of the sample and the detector in the beam path. If the detector is placed directly after the sample, a conventional absorption image is obtained. However, if the X-ray source is sufficiently small (thereby resulting in a source with high spatial coherence, since the spatial coherence scales as the inverse square of the spot size) and the detector is placed at a certain distance from the sample, then the near-field diffraction (Fresnel) condition is realized. Phase contrast is made observable by steep phase gradients and discontinuities (interfaces) in the object, which causes interferences resulting in intensity modulation in the image.

Recent advances in ultrafast laser technology could make the laboratory phase-contrast micro-tomography practical with a unique possibility of combining imaging with femtosecond technology. We demonstrate here that phase contrast imaging can be successfully realized with an ultrafast laser-based, compact, 300 fs duration X-ray source (Toth *et al.*, 2005).

Experiments have been conducted with the femtosecond Ti:sapphire laser presently available at the INRS. The peak and average power are 10 TW and 6 W, respectively. The repetition rate is 10 Hz and the energy obtained at 800 nm wavelength after compression is 600 mJ in 60 fs pulse with an energy stability of 3% rms. The prepulse-to-main pulse contrast ratio at the fundamental frequency is 1×10^{-6}. Phase front correction has been introduced on this system to control the transverse beam quality and the temporal shape. Laser diagnostics include single shot and third-order autocorrelators, frequency resolved optical gating (FROG), phase front sensor (Shack Hartman interferometer), and near and far field imaging.

The optical beam is frequency doubled by a KDP crystal. Using a KDP crystal (type I, 2 mm thickness) with fundamental pump intensity between 100 to 200 $GWcm^{-2}$, we were able to obtain conversion efficiencies of 40% from the fundamental beam to the second harmonics. The prepulse-to-main pulse contrast ratio at the second harmonic frequency is about 1×10^{-10}. The target is moved between two shots so that the beam interacts with a fresh flat surface at each shot.

Our X-ray imaging system allows a wide dynamic range (10^4 or greater) and fast readout with low electronic noise. For convenient coupling of scintillator screens to the CCD, a 1:1 fiber-optic faceplate is permanently bonded to the chip. This faceplate isolates the CCD, which is placed under vacuum to eliminate any condensation due to cooling. Thus, the presence of the fiber-optic faceplate with its 25 l p/mm resolution provides flexibility, while maintaining the intrinsic system resolution.

https://doi.org/10.1017/S0263034606060150 Published online by Cambridge University Press

Various test objects including low-density optical fibers, thin plastic edges, paper edges, contrast and mammographic phantoms, as well as biological samples have been imaged. The distance between the source and the object was maintained constant at 45 cm under vacuum, while the distance between the object and the detector was varied from 3 cm up to 180 cm in air.

Phase contrast images of complex objects have been obtained under the same experimental conditions. Figure 4 shows the phase-contrast image of a bee. These images were taken at X-ray photon fluxes between 5×10^7 to 5×10^9 photons cm^{-2}. One can clearly see the enhancement due to phase-contrast, a bright fringe emphasizing the interfaces in different parts of the bee (indicated by the arrows). Similar contrast enhancements are also observed in images of a thicker biological sample. The technique is already at a sufficient level for applications in imaging small mamallian animals. However, higher performance of the X-ray source, such as increased average power (by, for example, increase in the repetition rate of the pump laser), and optimization of the X-ray photon energy for each sample to be imaged, should greatly accelerate the application of the technique to various medical needs.

4. CONCLUSION

We have briefly presented the status of the ALLS, a state-of-the-art multi-beam Ti:sapphire laser system presently

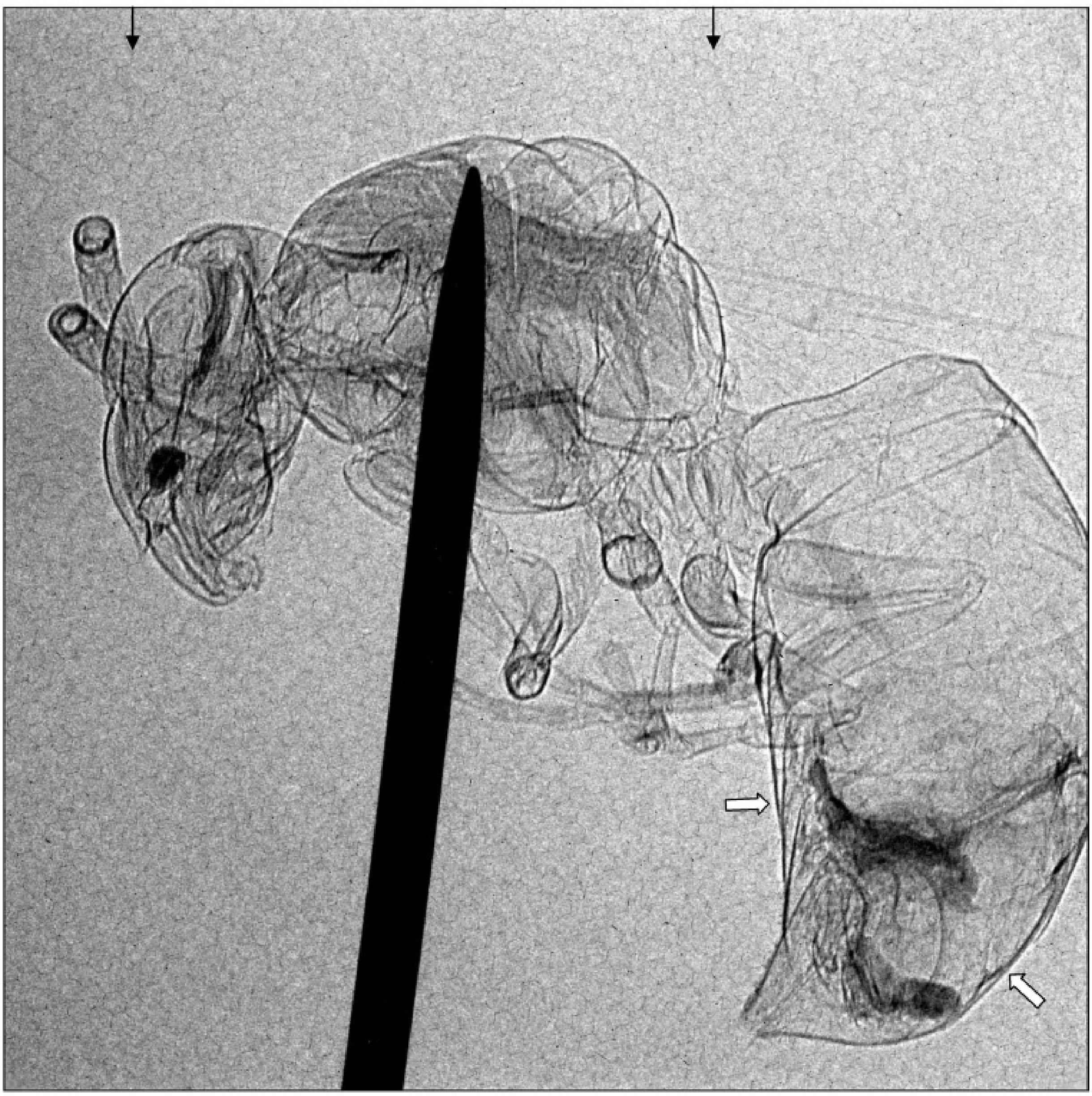

Fig. 4. Phase contrast projection images of a bee.

https://doi.org/10.1017/S0263034606060150 Published online by Cambridge University Press

under construction in Canada. The 25 fs ALLS multi-beam laser system has three components, each with different repetition rate and output energy. These multiple laser beams will be used to generate a "*rainbow*" of femtosecond pulses from the far infrared to hard X-rays, which can be combined to perform unique experiments, such as dynamic molecular imaging. We have described two examples of experiments that are planned by our group with the ALLS facility. The first is the observation of a plateau in the high-order harmonic generation (up to 53rd) using boron ablation medium is reported for the first time to our knowledge. The steep decrease of the intensity for low-order harmonics (up to 19th) was followed by plateau with conversion efficiencies in the range of 10^{-4} (for third harmonic) to 10^{-7} (at the plateau range). Harmonic generation appear to be efficient in the case of neutral plasma when ion and electron concentration were negligible.

We have also recently demonstrated the feasibility of femtosecond phase-contrast in-line imaging using ultrafast laser-based X-ray source. Enhanced image contrast using phase contrast has been successfully observed for otherwise low contrast objects and interfaces of a wide range of small test objects and biological samples, with exposure times between 10 s and a few minutes. Microtomography with our laser based X-ray source is also considered in the near future.

REFERENCES

Akiyama, Y., Midorikawa, K., Matsunawa, Y., Nagata, Y., Obara, M., Tashiro, H. & Toyoda, K. (1992). Generation of high-order harmonics using laser-produced rare-gas-like ions. *Phys. Rev. Lett.* **69**, 2176–2179.

Altucci, C., Starczewski, T., Mevel, E., Wahlström, C.-G., Carré B. & L'Huillier, A. (1996). Influence of atomic density in high-order harmonic generation. *J. Opt. Soc. B* **13**, 148–156.

Backus, S., Bartels, R., Thompson, S., Dollinger, R., Kapteyn, H.C. & Murnane, M.M. (2001). High-efficiency, single-stage 7-kHz high-average-power ultrafast laser system. *Opt. Lett.* **26**, 465–467.

Cerullo, G. & De Silvestri, S. (2003). Ultrafast optical parametric amplifiers. *Rev. Sci. Instrum.* **74**, 1–18.

Corkum, P. B. (1993). Plasma perspective on strong-field multiphoton ionization. *Phys. Rev. Lett*. **71**, 1994–1997.

Flettner, A., Pfeifer, T., Walter, D., Winterfeldt, C., Spielmann, C. & Gerber, G. (2003). High-harmonic generation and plasma radiation from water microdroplets. *Appl. Phys. B* **77**, 747–751.

Ganeev, R.A., Redkorechev, V.I. & Usmanov, T. (1997). Optical harmonics generation in low-temperature laser-produced plasmas. *Opt. Commun.* **135**, 251–256.

Ganeev, R.A., Kanai, T., Ishizawa, A., Ozaki, T. & Kuroda, H. (2004). Development and applications of a compact hybrid tabletop terawatt chirped-pulse amplification Ti:sapphire-Nd:glass laser for X-ray lasing and harmonic generation. *Appl. Opt.* **43**, 1396–1403.

Gavrilov, S.A., Golishnikov, D.M., Gordienko, V.M., Savel'ev, A.B. & Volkov, R.V. (2004). Efficient hard X-ray source using femtosecond plasma at solid targets with a modified surface. *Laser Part. Beams* **22**, 301–306.

Gureyev, T.E., Mayo, S., Wilkins, S., Paganin, D. & Stevenson A.W. (2001). Quantitative in-line phase contrast imaging with multienergy X-rays. *Phys. Rev. Lett.* **86**, 5827–5830.

Keller, U. (1994). Ultrafast all-solid-state laser technology. *Appl. Phys. B* **58**, 347–363.

Kuroda, H., Suzuki, M., Ganeev, R., Zhang, J., Baba, M., Ozaki, T., Wei, Z.Y. & Zhang, H. (2005). Advanced 20 TW Ti : S laser system for X-ray laser and coherent XUV generation irradiated by ultra-high intensities. *Laser Part. Beams* **23**, 183–186.

Limpouch, J., Klimo, O., Bina, V. & Kawata, S. (2004). Numerical studies on the ultrashort pulse K-alpha emission sources based on femtosecond laser-target interactions. *Laser Part. Beams* **22**, 147–156.

Macklin, J.J., Kmetec, J.D. & Gordon, C.L. III (1993). High-order harmonic generation using intense femtosecond pulses. *Phys. Rev. Lett.* **70**, 766–769.

Nisoli, M., Stagira, S., De Silvestri, S., Svelto, O., Sartania, S., Cheng, Z., Tempea, G., Spielmann, C. & Krausz, F. (1998). Toward a terawatt-scale sub-10-fs laser technology. *IEEE J. Sel. Top. Quantum Electron.* **4**, 414–420.

Norreys, P.A., Zepf, M., Moustaizis, S., Fews, A.P., Zhang, J., Lee, P., Bakarezos, M., Danson, C.N., Dyson, A., Gibbon, P., Loukakos, P., Neely, D., Walsh, F.N., Wark, J.S. & Dangor, A.E. (1996). Efficient extreme uv harmonics generated from picosecond laser pulse interactions with solid targets. *Phys. Rev. Lett.* **76**, 1832–1835.

Pascolini, M., Poletto, L., Sansone, G., Stagira, S., Vozzi, C., Nisoli, M., Villoresi, P., Tondello, G. & De Silvestri, S. (2004). Toward the single-cycle regime in the generation of high-order laser harmonics. *Laser Part. Beams* **22**, 335–339.

Reintjes, J.F. (1984). *Nonlinear Optical Parametric Processes In Liquids And Gases*. New York: Academic.

Seres, E., Seres, J., Krausz, F., Spielmann & C. (2004). Generation of coherent soft-X-ray radiation extending far beyond the titanium L edge. *Phys. Rev. Lett.* **92**, 163002.

Spielmann, C., Burnett, N.H., Sartania, S., Schnürer, M., Kan, C., Lenzner, M., Wobrauschek, P. & Krausz, F. (1997). Generation of coherent X-rays in the water window using 5-femtosecond laser pulses. *Science* **278**, 661–664.

Toth, R., Kieffer, J.C., Fourmaux, S., Ozaki, T. & Krol, A. (2005). In line phase contrast imaging with a laser-based hard X-ray source. *Rev. Sci. Instrum.* **76**, 083701.

Wilkins, S.W., Gureyev, T.E., Gao, D., Pogany A. & Stevenson, A.W. (1996). Phase contrast imaging using polychromatic hard X-rays. *Nature* **384**, 335–338.